A COMPARISON OF DNA DAMAGE PROBES IN TWO HMEC LINES WITH X-IRRADIATION

CHRISTY L. WISNEWSKI, KATHLEEN A. BJORNSTAD, CHRISTOPHER J. ROSEN, POLLY Y. CHANG, AND ELEANOR A. BLAKELY

ABSTRACT

In this study, we investigated γH2AX^{ser139} and 53BP1^{ser25}, DNA damage pathway markers, to observe responses to radiation insult. Two Human Mammary Epithelial Cell (HMEC) lines were utilized to research the role of immortalization in DNA damage marker expression, HMEC HMT-3522 (S1) with an infinite lifespan, and a subtype of HMEC 184 (184V) with a finite lifespan. Cells were irradiated with 50 cGy X-rays, fixed with 4% paraformaldehyde after 1 hour repair at 37ºC, and processed through immunofluorescence. Cells were visualized with a fluorescent microscope and images were digitally captured using Image-Pro Plus software. The 184V irradiated cells exhibited a more positive punctate response within the nucleus for both DNA damage markers compared to the S1 irradiated cells. We will expand the dose and time course in future studies to augment the preliminary data from this research. It is important to understand whether the process of transformation to immortalization compromises the DNA damage sensor and repair process proteins of HMECs in order to understand what is "normal" and to evaluate the usefulness of cell lines as experimental models.

INTRODUCTION

DNA damage from ionizing radiation triggers the mobilization of damage sensor proteins to damage sites resulting in temporary delay of cell cycle progression and activation of repair machinery (1). ATM (Ataxia Telangiectasia Mutated) and ATR (Ataxia Telangiectasia and Rad-3-related) proteins are two related kinases central to signaling DNA damage, and recent evidence

indicates ATM activation occurs prior to ATR activation following radiation damage (2). The published literature of these phenomena has been obtained primarily with human and other mammalian fibroblasts.

A major focus for breast cancer research is to understand the key mechanisms responsible for initiating carcinogenesis. It is the epithelial cell that becomes a cancer cell. Normal epithelial cells have a finite life span and then senesce, and thus are more difficult to study in the laboratory. Evidence exists from studies of human and murine normal mammary glands that multiple epithelial cell-subtypes exist with distinct patterns of susceptibility to different subtypes of breast cancer (3, 4, 5). Malignant transformation is a multi-step process in which genetic changes in these different cell subtypes can occur due to exposure to a number of environmental factors, such as viruses, carcinogens, dietary factors, and radiation. Mutations of the TP53 gene are the most frequent genetic lesion in breast cancer and its loss as a result of mutation is thought to be an early step in breast tumorigenesis (6).

Numerous cell culture models derived from Human Mammary Epithelial Cells (HMEC) are available (4, 7, 8). The role of tumor suppressor proteins, inhibitors of cyclin-dependent kinases, telomerase and small G proteins have been defined in normal and various stages in the progression to immortalization of HMECs. In this paper we are investigating whether DNA damage foci recruitment after exposure of HMECs to a relatively low dose of X-rays (50 cGy) is dependent on immortalization. We have selected two non-malignant HMECs: the 184V non-immortalized HMEC with a finite life span, and the immortalized HMEC HMT-3522 (S1) (9, 10, 11, 12). Differences in gene expression between these two cell types during normal differentiation into polarized acini have recently been compared to test correlation of marker genes with poor and good prognosis groups among breast cancer patients (13).

We are comparing two markers in the ATM DNA damage pathway for radiation-induced effects, histone family 2A member X (γH2AX), and tumor protein TP53 binding protein 1 (53BP1) (14, 15). Both proteins are phosphorylated in response to DNA damage (16, 17, 18). We hypothesize that the transformation process that immortalizes cells for unlimited growth in culture may affect the DNA damage response pathway. Biological cell models cultured *in vitro* in the laboratory are used to investigate many unknown mechanisms of action underlying molecular responses to stressors in normal human tissues. It is important to understand biological characteristics common to a cell type, as well as differences that may exist in various cell models.

MATERIALS AND METHODS

Cells and Cell Culture Conditions

HMEC HMT-3522 (S1) immortalized cells are non-malignant early passage human cells that were made available to our lab by Drs. Mina Bissell and Mary Helen Barcellos-Hoff (LBNL). The cells originated from a reduction mammoplasty of a woman with a non-malignant breast lesion and were derived through continuous cell passaging in defined medium (20, 21). We used cells from passages #40-60. Cells were grown at 37^{o}C in humidified incubator at 5 % CO_2 in a chemically-defined medium (DMEM / F12 - H14) composed of DMEM (Dulbecco's Modified Eagle's Medium) plus Ham's F12 (1:1, Invitrogen), 2 mM glutamine, 250 ng/ml insulin, 5 mg/ml sheep prolactin, 10 mg/ml transferrin, 10^{10} M estradiol (all from Sigma, St. Louis, MO), 10 ng/ml EGF, 2.6 ng/ml sodium selenite, and 1 μM hydrocortisone (from Collaborative Research, MA). Cells were set up in plastic four well LabTek slides or 60 mm plastic Falcon petri dishes at 4 x 10^4 cells/well or 1x10^5 respectively five days prior to the experiment and were fed every other day.

HMEC 184V is a subtype of the 184 HMEC line that is mortal and non-malignant. These cells were kindly provided by Dr. Martha Stampfer (LBNL), who developed this cell line from a human non-tumorigenic reduction mammoplasty (10, 19). Cells were grown as described by Stampfer (19) in serum-free MCDB 170+IP Growth Media containing MEBM, (Mammary Epithelial Basal Medium, Clonetics Corporation, San Diego, CA) in a 37°C humidified incubator at 0.2% CO_2. 184V cells were fed every Monday, Wednesday, and Friday, and transferred at 80% confluency. Cell transfer consisted of 3X rinses of 0.05% trypsin w/ EDTA (Invitrogen/GIBCO) of 3, 2, and 1 ml, respectively, in 100 mm petri dishes. The 184V cells required waiting 30 seconds between trypsin rinses, with the final trypsinization for 5 minutes at 37°C. Following the final trypsinization, cells were neutralized (with 10 ml 1X PBS without Ca or Mg) and spun down in a centrifuge at 1,000 RPM for 5 minutes. Cells were resuspended in growth media, counted, and plated. Cells were plated at 2-4 x 10^4 cells/ml per well into plastic four well LabTek slides three days prior to the experiment.

Irradiation

Four well LabTek slides and 60 mm petri dishes were irradiated one at a time, on a rotating platform, in a 160 kVp Pantak X-ray machine, running at 150 kVp, 20 mA, for a dose of radiation of 50 cGy. Dose calibration was done with a NIST-based calibrated Victoreen probe 154. Following irradiation, slides or dishes containing S1 or 184V HMECs were incubated at 37°C at 5.0% and 0.2% CO_2, respectively, until fixation.

Fixation

Cells were fixed following irradiation, at 1 hour. Cells were rinsed 2X with PBS and then incubated with Nucleoplasmic Extraction Solution (NES): 0.5% Triton-X, 20 mM HEPES (pH 7.9), 50 mM NaCl, 3 mM $MgCl_2$, and 200 mM sucrose at RT for 10 minutes. The cells

were rinsed 1X with PBS and fixed with 4% paraformaldehyde for 10 mins at RT in a time course after radiation exposure. Cells were rinsed 2X with PBS, and then PBS was added to each area of the slide/dish containing cells, and placed at 4°C overnight.

Immunofluorescence

Cells fixed with 4% paraformaldehyde were permeabilized in 0.1% NP-40 in PBS for 30 minutes. Cells were blocked with 0.5% casein in PBS for 1 hour, followed by 10% goat serum in PBS for 1 hour. The primary antibodies for $\gamma H2AX^{ser139}$ monoclonal mouse (1:1000 Upstate) or $53BP1^{ser25}$ polyclonal rabbit (1:200 Bethyl Labs) were applied overnight at 4°C in a humidified chamber.

Cells were rinsed 3X 20 minutes in PBS, and secondary antibody was applied. Alexa 488 goat anti-mouse (1:300 Invitrogen) or Alexa 594 goat anti-mouse (1:300 Invitrogen) was applied for 1 hour for the S1 or 184V cells, respectively, for $\gamma H2AX^{ser139}$. Alexa 488 goat anti-rabbit (1:300 Invitrogen) or Alexa 594 goat anti-rabbit (1:300 Invitrogen) was applied for 1 hour for the 184V or S1 cells, respectively, for $53BP1^{ser25}$. Alexa 488 produces a green fluorescent signal and Alexa 594 produces a red fluorescent signal.

Cells were rinsed 3X 15 minutes in PBS, followed by nuclear staining in DAPI (0.25 μg/ml) for 5 minutes (nucleus stains blue) covered with vectashield, cover-slipped and sealed with nail polish.

Image Acquisition

A Zeiss Axiovert 200M microscope was used to view fluorescent cell signals which were digitally captured with a 40XAPO objective and a QImaging Retiga EX digital CCD camera. Image-Pro Plus software was used to acquire individual 40X images. A minimum of five images from each experimental condition were taken.

Fluorescence Analysis

The number of fluorescent cells was manually counted for each image field. The fraction of responders in the field was obtained by dividing the number of positive fluorescent nuclei divided by the total number of cells indicated by the blue DAPI stained nuclei. A minimum of 5 images from each sample were analyzed and the data is summarized in Table 1.

RESULTS

A representative fluorescent image from the 5 fields acquired from each 50 cGy irradiated sample after 1 hour of incubation at 37°C, and its respective control for each of the two DNA damage marker proteins with each cell type is depicted in Figure 1A for the $\gamma H2AX^{ser139}$ response, and in Figure 2A for the $53BP1^{ser25}$ response. A histogram representing the quantitative analysis of the fraction of the fluorescence positive cells for the $\gamma H2AX^{ser139}$ response is presented in Figure 1B and for the $53BP1^{ser25}$ in Figure 2B. About 20% of the unirradiated control samples for the exponentially-growing S1 cells or 184V cells were measured to be $\gamma H2AX^{ser139}$ positive. Although a comparable number of background positive cells were seen for each of the cell types, the nature of the fluorescence was quite different. Most of the signals from the S1 control samples were punctuate in nature while some 184V cells showed a distribution of both overall nuclear staining as well as punctuate signals. Both cell lines showed increased fluorescent signals one hour after an X-ray dose of 50 cGy, but the fluorescent signals had a different appearance. Most of the positive S1 cells showed global nuclear staining while signals from the 184V cells appeared to contain a distribution of both punctuate and overall nuclear staining. Quantitative comparison of the number of positive cells in the DAPI merged H2AX images showed that 91.6 ± 9.7% of the 184V cell nuclei were positive compared to the

83.4 ± 15.8% positive S1 cells. This is illustrated in the histograms in Figure 1B. Error bars show the standard deviation between image fields for the same probe and treatment condition.

In Figure 2A, the unirradiated S1 cells showed a very small background signal for 53BP1^{ser25} fluorescence. In stark contrast, the 184V cells showed a high background signal of small punctate dots. Both cell types showed increased 53BP1^{ser25} fluorescence 1 hour after exposure to 50 cGy. Quantitation of the fluorescence signal indicated that 97.8 ± 2.7% of the 184V cells were fluorescence positive, but only 69.2 ± 12.5% of the S1 cells were positive. Results from a student t-test show that the radiation-induced increase in fluorescence in the 184V cells are significantly different ($p<0.01$) than the S1 cells.

DISCUSSION AND CONCLUSIONS

The major observation from the work presented here is that the control background fluorescent signals for the two molecular markers used as indicators for radiation damage are different for the two non-malignant HMECs studied. Furthermore, although it appears that radiation exposure produced a similar level of enhanced γH2AX^{ser139} fluorescent signals in both cell lines, we observed significant differences in both the level and in the pattern of radiation-induced 53BP1^{ser25} fluorescence signal. The non-immortalized 184V HMECs showed almost 100% response 1 hour after exposure to 50 cGy with each of the two probes, γH2AX^{ser139} and 53BP1^{ser25}. The immortalized HMT-3522 S1 HMECs showed only approximately 70% 53BP1 response 1 hour after exposure to 50 cGy. To our knowledge, this work represents the first documentation of differences in DNA repair markers between two non-malignant HMECs.

Both cell types were exponentially dividing cultures at the time of radiation exposure. One explanation for the observed differences could be due to variable distributions of cells in the cell cycle for each cell type. However, the magnitude of this difference seems unlikely to

account for this possibility, but this needs to be ruled out in future studies by examining the cell cycle distribution. The data presented are for a single radiation dose and time point after exposure. It is therefore possible that the time course of the expression of these DNA damage markers is different for each of these cell lines. This would be an interesting observation and future work with a more complete dose response and time course is planned. It is known that multiple genetic changes are required for efficient immortalization of different subtypes of normal human mammary epithelial cells leading to carcinogenesis (4) and that some of these genetic changes can alter the radiation resistance of carcinoma of the breast (22). There are indications that DNA damage markers like $\gamma H2AX^{ser139}$ can be used as therapeutic targets for improving the efficacy of radiation therapy for breast cancer (23) by blocking γH2AX foci formation or by inhibiting DNA damage repair processes in breast tumor cells. It is important to understand whether the process of transformation to immortalization compromises the DNA damage sensor and repair process proteins of HMECs in order to understand what is "normal" and to evaluate the usefulness of cell lines as experimental models.

ACKNOWLEDGEMENTS

I would like to thank the U.S. Department of Energy, Office of Science for allowing me to participate in this magnificent undergraduate internship research experience within the SULI program. I want to thank the CSEE staff and coordinator Laurel Egenberger. Special thanks go to my mentors Eleanor Blakely, Kathleen Bjornstad, Polly Chang and Chris Rosen for their guidance and patience with my research project and for their immeasurable assistance with the research presented here. I would also like to thank Martha Stampfer, Al Thompson, Jim Garbe, Sylvain Costes, and Ekaterina Bassett for their knowledge regarding different aspects of this research. This work was supported by the Director, Office of Science, Office of Science

Education and Workforce Development, of the U.S. Department of Energy under Contract No. DE-AC02-05CH11231. In addition, this work was supported by the U.S. DOE's Low Dose Radiation Research Program under Contract No. DE-AC03-76SF00098 and the Center for Science and Engineering Education.

REFERENCES

[1] Kurz, EU and Lees-Miller, SP, "DNA damage-induced activation of ATM and ATM-dependent signaling pathways," *DNA Repair (Amst),* vol. 3, pp. 889-900, 2004.

[2] Adams, KE, Medhurst, AL, Dart, DA, and Lakin, ND, "Recruitment of ATR to sites of ionising radiation-induced DNA damage requires ATM and components of the MRN protein complex," *Oncogene,* vol. 25, pp. 3894-904, 2006.

[3] Band, V, "Preneoplastic transformation of human mammary epithelial cells," *Semin Cancer Biol,* vol. 6, pp. 185-92, 1995.

[4] Ratsch, SB, Gao, Q, Srinivasan, S, Wazer, DE, and Band, V, "Multiple genetic changes are required for efficient immortalization of different subtypes of normal human mammary epithelial cells," *Radiat Res,* vol. 155, pp. 143-150, 2001.

[5] Dimri, G, Band, H, and Band, V, "Mammary epithelial cell transformation: insights from cell culture and mouse models," *Breast Cancer Res,* vol. 7, pp. 171-9, 2005.

[6] Liu, FS, Yang, HY, and Sui, GJ, "The metastatic pattern of malignant tumors," *Zhonghua Yi Xue Za Zhi,* vol. 74, pp. 406-9, 454, 1994.

[7] Taylor-Papadimitriou, J, D'Souza, B, Berdichevsky, F, Shearer, M, Martignone, S, and Alford, D, "Human models for studying malignant progression in breast cancer," *Eur J Cancer Prev,* vol. 2 Suppl 3, pp. 77-83, 1993.

[8] Stampfer, MR and Yaswen, P, "Culture models of human mammary epithelial cell transformation," *J Mammary Gland Biol Neoplasia,* vol. 5, pp. 365-78, 2000.

[9] Hammond, SL, Ham, RG, and Stampfer, MR, "Serum-free growth of human mammary epithelial cells: rapid clonal growth in defined medium and extended serial passage with pituitary extract," *Proc Natl Acad Sci U S A,* vol. 81, pp. 5435-9, 1984.

[10] Stampfer, MR and Bartley, JC, "Induction of transformation and continuous cell lines from normal human mammary epithelial cells after exposure to benzo[a]pyrene," *Proc Natl Acad Sci U S A,* vol. 82, pp. 2394-8, 1985.

[11] Petersen, OW, Ronnov-Jessen, L, Howlett, AR, and Bissell, MJ, "Interaction with basement membrane serves to rapidly distinguish growth and differentiation pattern of normal and malignant human breast epithelial cells," *Proc Natl Acad Sci U S A,* vol. 89, pp. 9064-8, 1992.

[12] Weaver, VM, Petersen, OW, Wang, F, Larabell, CA, Briand, P, Damsky, C, and Bissell, MJ, "Reversion of the malignant phenotype of human breast cells in three-dimensional culture and in vivo by integrin blocking antibodies," *J Cell Biol,* vol. 137, pp. 231-45, 1997.

[13] Fournier, MV, Martin, KJ, Kenny, PA, Xhaja, K, Bosch, I, Yaswen, P, and Bissell, MJ, "Gene expression signature in organized and growth-arrested mammary acini predicts good outcome in breast cancer," *Cancer Res,* vol. 66, pp. 7095-102, 2006.

[14] Fillingham, J, Keogh, MC, and Krogan, NJ, "γH2AX and its role in DNA double-strand break repair," *Biochem Cell Biol,* vol. 84, pp. 568-577, 2006.

[15] Iwabuchi, K, Hashimoto, M, Matsui, T, Kurihara, T, Shimizu, H, Adachi, N, Ishiai, M, Yamamoto, K, Tauchi, H, Takata, M, Koyama, H, and Date, T, "53BP1 contributes to survival of cells irradiated with X-ray during G1 without Ku70 or Artemis," *Genes Cells,* vol. 11, pp. 935-48, 2006.

[16] Crawford, LV, Pim, DC, Gurney, EG, Goodfellow, P, and Taylor-Papadimitriou, J, "Detection of a common feature in several human tumor cell lines--a 53,000-dalton protein," *Proc Natl Acad Sci U S A,* vol. 78, pp. 41-5, 1981.

[17] Rogakou, EP, Pilch, DR, Orr, AH, Ivanova, VS, and Bonner, WM, "DNA double-stranded breaks induce histone H2AX phosphorylation on serine 139," *J Biol Chem,* vol. 273, pp. 5858-68, 1998.

[18] Mochan, TA, Venere, M, DiTullio, RA, Jr., and Halazonetis, TD, "53BP1 and NFBD1/MDC1-Nbs1 function in parallel interacting pathways activating ataxia-telangiectasia mutated (ATM) in response to DNA damage," *Cancer Res,* vol. 63, pp. 8586-91, 2003.

[19] Stampfer, MR, "Isolation and growth of human epithelial cells," *Journal of Tissue Culture Methods,* vol. 9, pp. 107-115, 1985.

[20] Briand, P, Nielsen, KV, Madsen, MW, and Petersen, OW, "Trisomy 7p and malignant transformation of human breast epithelial cells following epidermal growth factor withdrawal," *Cancer Res,* vol. 56, pp. 2039-44, 1996.

[21] Briand, P, Petersen, OW, and Van Deurs, B, "A new diploid nontumorigenic human breast epithelial cell line isolated and propagated in chemically defined medium," *In Vitro Cell Dev Biol,* vol. 23, pp. 181-8, 1987.

[22] Jameel, JKA, Rao, VSR, Cawkwell, L, Drew, "Radioresistance in carcinoma of the breast" *The Breast,* vol 13, pp 452-460, 2004.

[23] Kao, J, Milano, MT, Javaheri, A, Garofalo, MC, Chmura, SJ, Weichselbaum, RR, Kron, SJ, "γ-H2AX as a therapeutic target for improving the efficacy of radiation therapy" *Current Cancer Drug Targets,* vol 6, pp. 197-205 2006.

TABLE

HMEC Line	Antibody	Cells Counted					
		Control			1 hr post 50 cGy X-ray		
		+	Total	%	+	Total	%
S1	γH2AX^{ser139}	56	257	22.0 ± 8.1%	405	490	83.4 ± 15.8%
	53BP1^{ser25}	2	323	0.7 ± 0.1%	353	524	69.2 ± 12.5%
184V	γH2AX^{ser139}	78	329	24.1 ± 7.2%	336	368	91.6 ± 9.7%
	53BP1^{ser25}	230	298	77.9 ± 15.8%	359	368	97.8 ± 2.7%

Table 1. Data and calculated percentages for cells counted

FIGURE CAPTIONS

Figure 1A. $\gamma H2AX^{ser139}$ response in control (a, b, e, f) and 50 cGy (c, d, g, h) images for HMEC S1 (a-d) and HMEC 184V (e-h). Panels a, c, e, g consist solely of the red signal from $\gamma H2AX^{ser139}$ and panels b, d, f, h are color composite images derived from merging the blue DAPI nuclear and the red $\gamma H2AX^{ser139}$ images.

Figure 1B. Comparison of the level of positive $\gamma H2AX^{ser139}$ in control or irradiated cell populations, in HMECs S1 or 184V.

Figure 2A. $53BP1^{ser25}$ response in control (a, b, e, f) and 50 cGy (c, d, g, h) images for HMEC S1 (a-d) and HMEC 184V. Panels a, c, e, g consist solely of the green signal from $53BP1^{ser25}$ and panels b, d, f, h are color composite images derived from merging the blue DAPI nuclear and the green $53BP1^{ser25}$ images.

Figure 2B. Comparison of the level of positive $53BP1^{ser25}$ in control or irradiated cell populations of HMECs S1 or 184V.

FIGURES

Figure 1A.

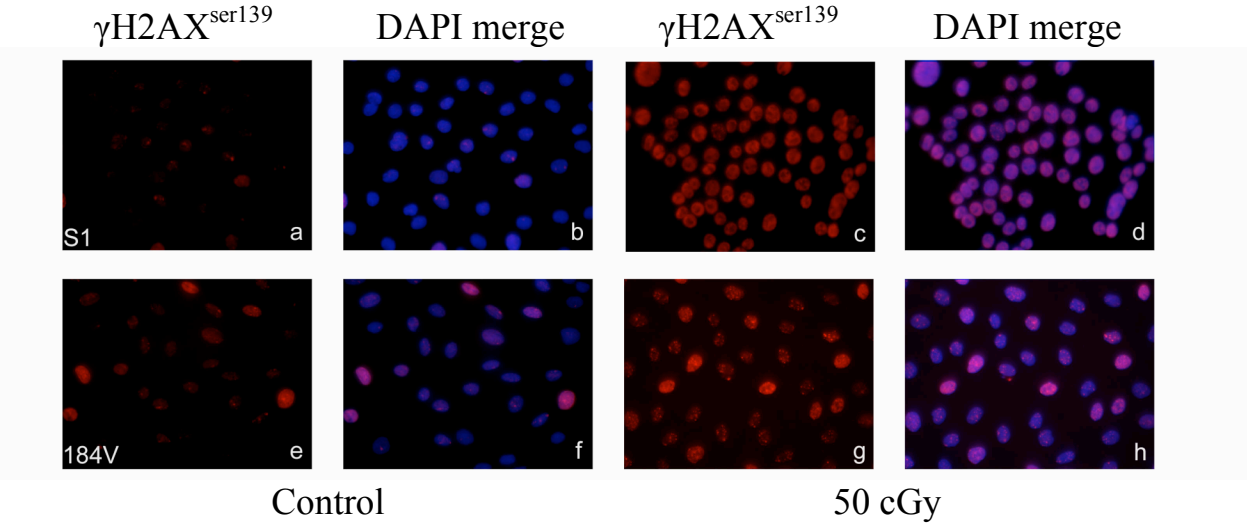

Figure 1B.

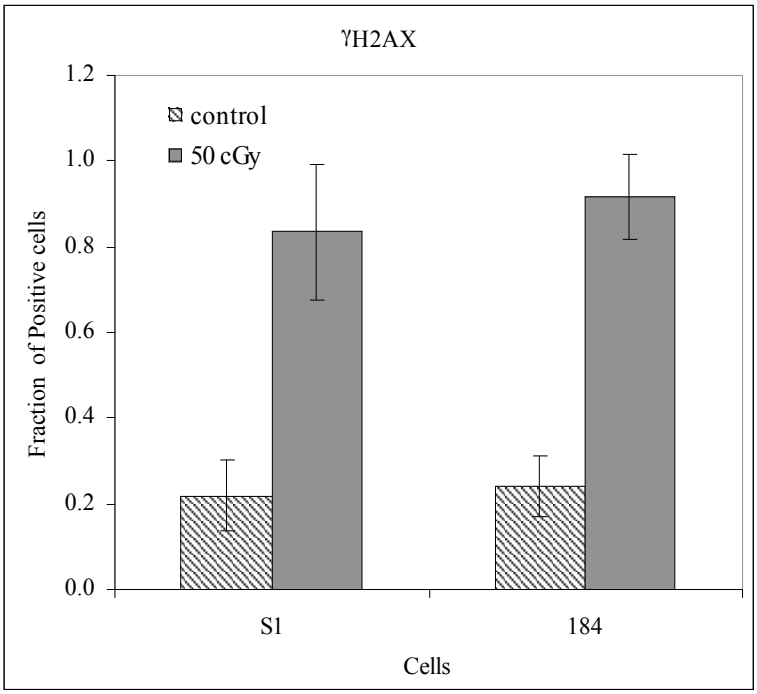

Figure 2A.

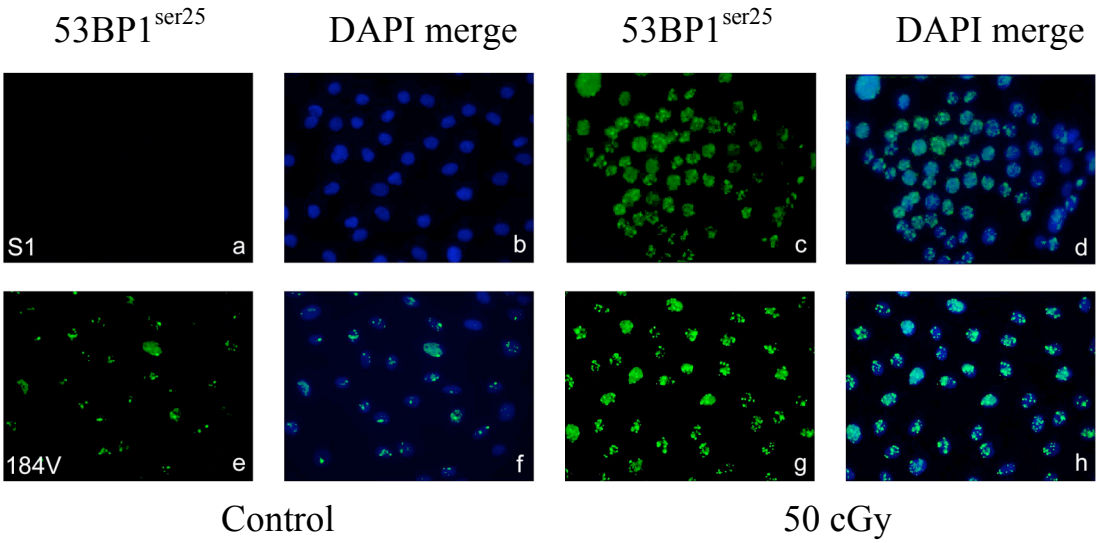

Figure 2B.